


## Analysis of dilution response surfaces and bead morphology in MIG-welding process

 <https://doi.org/10.56238/sevned2024.010-051>

Rafael Ellwanger Pimentel<sup>1</sup>, Arnaldo Ruben Gonzalez<sup>2</sup>, Matheus Botega<sup>3</sup> and Leandro Rubén González<sup>4</sup>

### ABSTRACT

The complexity of the current welding processes, as well as their sensitivity and precision, make it necessary to use statistical methods and optimization, accompanied by the search for experimental error and the adjustment of the model obtained, aiming at reducing time and cost. Although there are numerous treatments that have emerged over time, the Response Surface Methodology (MSR) has become one of the most appropriate ways to manage research related to this scope, by combining design and analysis of experiments, modeling and optimization. In addition, the search for processes that adjust to the needs imposed in the current scenario for coating, leads to the research of new welding processes, which combine low dilution, with maximized reinforcement width and height values, with only one layer. This difficulty causes welding processes to be conducted in conjunction with these tools, making the process more efficient. In this sense, with the objective of joining the two fronts exposed, the present work, through the use of Box-Behnken (BBD), sought to analyze the MSR of the dilution, width and height of reinforcement, with the use of MIG-PV welding, with filler metal AWS A5.9 ER385 (analogous to AISI 904L) in position (1G) on free surface (bead-on-plate) on ASTM A36 carbon steel substrate, with a thickness of 6.35 mm, in addition to optimizing the process via desirability with reinforcement height. The result showed that the input values were adjusted, considering the R<sup>2</sup> values of 88%, as well as the morphology of the surfaces. In addition, it showed maximum desirability in optimization, with an experimental error of 8.8%, with average height values of 5.2 mm, having great application in the current industry, with only one layer.

**Keywords:** Welding, Cladding, BBD, MSR, Dilution, Optimization.

---

<sup>1</sup> Doctor student in Mechanical Engineering, UFRGS, Porto Alegre, Rio Grande do Sul, Brazil.

E-mail: rafaellpimentel@hotmail.com

<sup>2</sup> Doctor in Mining, Metallurgical and Materials Engineering, UFRGS, Porto Alegre, Rio Grande do Sul, Brazil.

E-mail: ruben@mecanica.ufrgs.br

<sup>3</sup> Master's student in Mechanical Engineering, UFRGS, Porto Alegre, Rio Grande do Sul, Brazil.

E-mail: matheusbotega94@gmail.com

<sup>4</sup> Master's student in Mechanical Engineering, UFRGS, Porto Alegre, Rio Grande do Sul, Brazil.

E-mail: leorubengonzalez@gmail.com

## INTRODUCTION

The Response Surface Methodology (MSR) encompasses a structure, tool or technique, of great application and potential for modeling and optimization of industrial processes. This is proven by the large number of studies in various areas of knowledge, such as engineering (GHAEDI et al., 2015), health (Augustin et al., 2012), and manufacturing (ROSHAN ET AL., 2013). Analyzing specific welding applications, the topic becomes a range of possibilities, since it is possible to find numerous welding processes that are analyzed through MSR (AHMADNIA ET AL., 2016; HASAN ET AL., 2017; JAHANZAIB ET AL, 2017; LOTFI AND NOUROUZI, 2014; MOSTAAN ET AL., 2016; MOSTAFAPOUR ET AL., 2017; KORRA ET AL., 2015; RAMACHANDRAN ET AL., 2016; SAFEEN ET AL., 2016; SHI ET AL., 2014; WINICZENKO, 2016).

However, as the analyzed terms can carry a certain complexity, it is necessary to correctly design the proposed experiment, since the application makes the initially analyzed region delimited (MYERS and MONTGOMERY, 2009), and the input variables end up controlling the output variables (MONTGOMERY, 2017). Evidently, the relationship of these variables within the experimental arrangement is dictated by statistical concepts derived from mathematics (LEITHOLD, 1994). However, depending on the variables involved and their quantities in practical cases of everyday life, even with this numerical support, the functions of interest may still be unknown (BOX, 1954; STEWART, 2012).

The knowledge of the set of variables that govern the experiment ends up implying the search for oriented procedures to be able to evaluate the effect of this variation on the output variables of the proposed study (MONTGOMERY, 2017). Therefore, and in response to this need, numerous techniques have been developed to circumvent this problem, which end up forming the study of Experiment Planning and Analysis (DoE), and which stands out the Central Compound (CCD), Box-Behnken (BBD), Taguchi. The choice of these arrangements is decided depending on the need for application, and can be evaluated on several fronts, and be used individually (EKICI AND MOTORCU, 2014; TEIMOURI ET AL., 2017), in combination (PATEL ET AL., 2016) or even comparatively (SIVARAOS ET AL., 2014), sometimes seeking a better refinement of the process.

The use of this tool is not separate from its correct interpretation. In addition to due space constraints, either by the initial arrangement or by a reallocation of points with the aim of achieving the expected response, the determination of the choice of input variables becomes important, and presents two methods practiced: the first, more traditional, is employed a fractional arrangement with few runs (BOX AND HUNTER, 1961), and in the other, there is a readjustment of values similar to those of the literature, together with a baggage of practical experience of the person responsible (GOOS AND JONES, 2011), and there may also be an initial exploratory project.

However, the analysis and understanding of the convexity of the response surface, the curvature and the relationship of the direction of optimization are fundamental (HOERL, 1985) since a concave surface has a minimum point, and a convex maximum point. However, some response morphologies may have a saddle-shaped geometry, which sometimes makes it difficult to obtain maximum points, if not minimum points, and are commonly seen in manufacturing processes (SENTHILKUMAR AND KANNAN, 2015; VERMA ET AL., 2017).

Optimization turns out to be a variant of the MSR itself, being a component of the methodology. It can be understood as a necessary attribute to be objectified according to the nature of the problem (RAO, 2009; ZAVADSKAS AND TURSKIS, 2010). Depending on the morphology of the response, a rational direction can be assigned, looking for minimum, maximum or even target values, to then characterize the new input variables (DEB ET AL., 2017; ŠAPARAUSKAS ET AL., 2011), thus finding the equation of response and experimental error (BRIGHTMAN, 1978).

In the manufacturing area, it is easy to find work that maximizes results, especially in welded alloys, for example, increasing tensile strength (KUMAR ET AL., 2017; SUDHAGAR ET AL., 2017). On the other hand, studies on machined parts aimed at reducing the roughness of the parts, seeking, of course, minimum response values (KANT AND SANGWAN, 2014; ÖKTEM ET AL., 2005). The subject does not cease, since numerous studies can be analyzed with the objective of seeking the optimization of maximum and minimum values (ABUHABAYA ET AL., 2013; SONG ET AL., 2014).

A method of optimization of the response surface is the *desirability*, or desirability, initially proposed by (DERRINGER AND SUICH, 1980), which, through the simple and compound desirability values, returns the values sought as minimum, maximum or target, always observing the morphology of the response, the interaction of the optimization and its desirability values. Welding works apply the method (AHMADNIA ET AL., 2016, PIMENTEL, 2023; PIMENTEL ET AL., 2023) as well as being applied in other processes (HOSSEINZADEH AND MOUZIRAJI, 2016), showing its importance.

In welding processes, there is often a need to use the tool, due to the difficulties of the parameters involved. In the study, the application of the analysis of the response surface of the input variables and the relationship with the output variables is proposed. Graphs of dilution responses, an important variable in the welding process, especially in cladding applications, were plotted (GOMES, 2010; PIMENTEL, 2023; PIMENTEL ET AL., 2023). In addition, the morphology of the bead was analyzed, such as its width (L) and reinforcement height (H), which are important parameters for welding application (PIMENTEL ET AL., 2023).

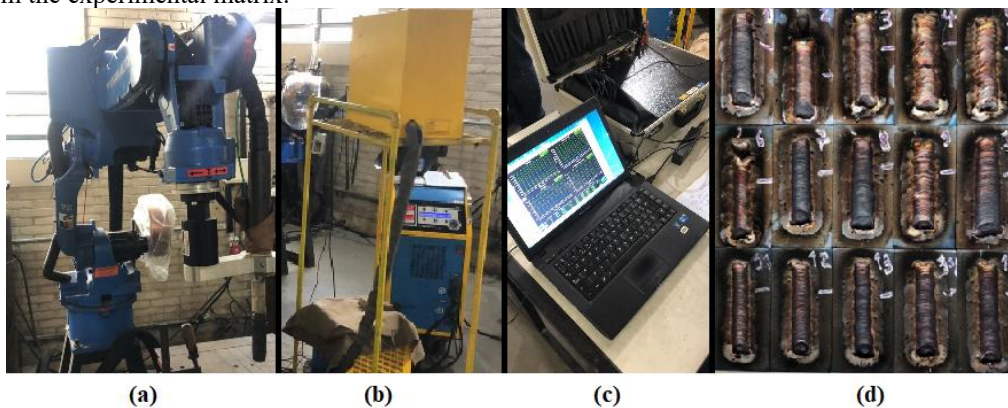
In addition, it was proposed the optimization of the experimental arrangement via the desirability method with maximum reinforcement height value, since they impact on the morphology

of the coating. To this end, the MIG/MAG-PV process was used, which, due to its reverse polarity, can achieve the necessary application for coating, since it reduces the temperature and better controls the process (FARIAS ET AL., 2005; PUHL, 2011). The process was deposited as a coating with the addition of AWS A5.9 ER385 wire (analogous to AISI 904L) on ASTM A36 carbon steel plates.

## MATERIALS AND METHODS

The MIG-PV welding procedure and analysis were carried out at the Laboratory of Welding & Related Techniques (LS&TC) of the Federal University of Rio Grande do Sul. The equipment used for welding and data collection and the experimental matrix are shown in Figure 1. To drive the torch the Yaskawa robotic arm (a), an IMC DIGIPlus A7 450 welding source and wire feeding device (b), an IMC SAP V4.01 portable data acquisition and process control system (c), and the fifteen deposited strands of the experimental matrix (d).

Figure 1:(a) Robotic arm; (b) welding source and wire feeding system; (c) data acquisition system; (d) fifteen strands deposited from the experimental matrix.



The MIG/MAG – PV process was used with filler metal AWS A5.9 ER385 (analogous to AISI 904L) in position (1G) on a *bead-on-plate* on ASTM A36 carbon steel substrate, with dimensions 150 x 50 x 6.35 mm. In addition, the process was carried out with weaving, where studies have shown good results (FRATARI ET AL., 2010; MIRANDA ET AL., 2015). The levels of the input factors can be seen in Table 1, and were used in the Box-Behnken (BBD) design of experiments, for three factors it requires only 12 executions and three more replicates at the central point, totaling 15 executions (BOX AND BEHNKEN, 1960). In addition to the application of BBD, the response surface method was employed, which, analogous to the graphical representation of a cube for the BBD, results in the graphical representation of the surface of the result that can be optimized (BOX AND DRAPER, 1987).

Table 1: Input parameters and levels of the applied experiment design.

Factors	Levels		
	Minimum value (-1)	Center Point (0)	Maximum value (+1)
Amplitude (mm): <b>At</b>	6,0	7,0	8,0
Weaving Frequency (Hz): <b>Ft</b>	0,6	0,9	1,2
Welding speed (mm/s): <b>Vs</b>	1,5	2,0	2,5

The parameters of the variable polarity current curve were obtained through previous tests, but also by analyzing and changing the parameters of past studies, since good initial results were not obtained (KANNAN AND YOGANANDH, 2010; MURUGAN AND PARMAR, 1994; NASCIMENTO ET AL., 2009). The values can be seen in Table 2, as well as other values kept constant throughout the welding process, in addition to the filler metal diameter of 1.2 mm, can be observed: torch travel angle (neutral) = 0 °, part-contact nozzle distance (DBCP) = 18 mm, shielding gas flow rate (argon) = 18 l/min.

Table 2: Parameters Held Constant of the Variable Polarity Current Curve.

Current Curve Parameters	Constant values
Ip - Positive Peak Running	350 A
Tp – Positive Peak Time	3.0 ms
Ib - Base Running	40 A
Tb - Base time	5.0 ms
In - Negative pico current	-70 A
Tn – Negative Peak Time	5.0 ms

The welding procedure consisted of the deposition of a bead on each plate, totaling 15 experiments plus two plates for reinforcement height validation by the optimization method. For the experimental error, the simple average of two cords was performed. The cross-sections, after being cut with a standard (*cut-off*) machine, available in the laboratory, were embedded, sanded and polished. Afterwards, the attack with the chemical reagent Nital 2% was used to develop the macrographs.

In addition, the images were obtained using the Leica EZ4 HD magnifying glass and the measurements were taken using the free *software* ImageJ, with a simple average of three checks. The *software* used for the analysis of the experiment and plotting the graphs was Minitab® and Statistica®,

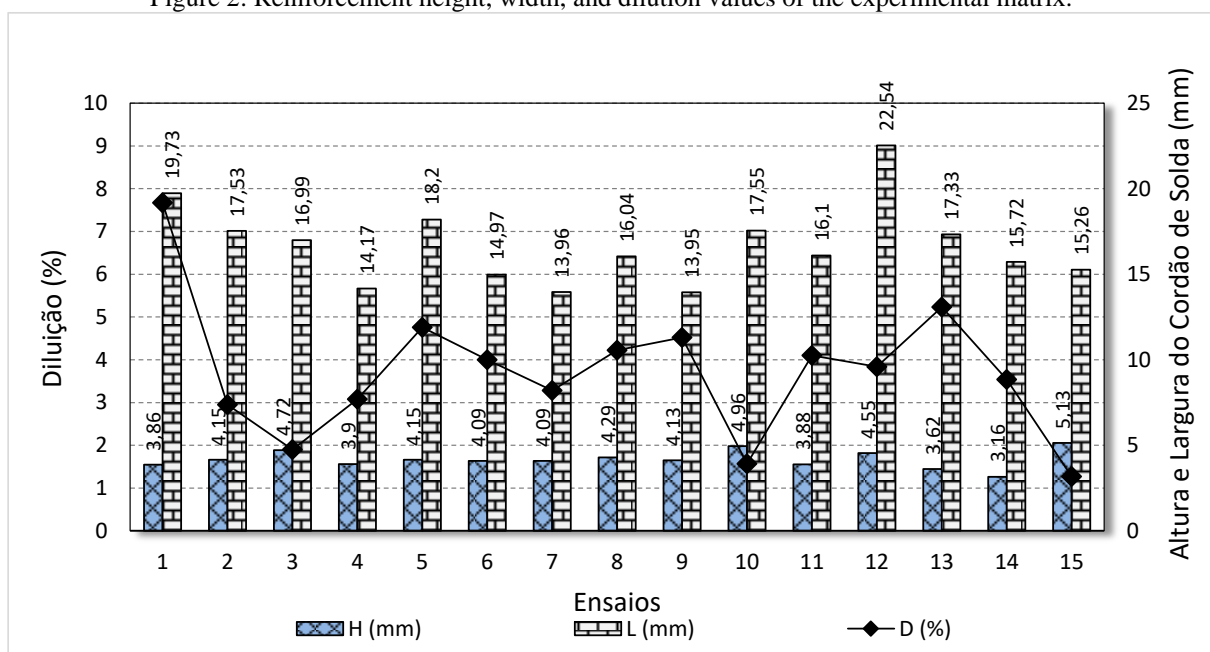
made available by the university. Surface graphs of dilution response, as well as reinforcement height and width were generated.

Analysis of variance (ANOVA) was used to evaluate the main effects (linear and quadratic) and interactions of the factors on the observed responses. For this analysis, a confidence level ( $\alpha$ ) of 0.05 was used, and for alpha values ( $\alpha$ ) lower than 5%, it was assumed that the control variable in question is significant in the response. The term p-value is known for the probability of significance, if it presents values higher than 0.05 (5%), the null hypothesis (factor is not significant) can be rejected with 95% confidence. However, the lower the p-value value, the greater the influence of the parameter on the analyzed response.

## RESULTS AND DISCUSSIONS

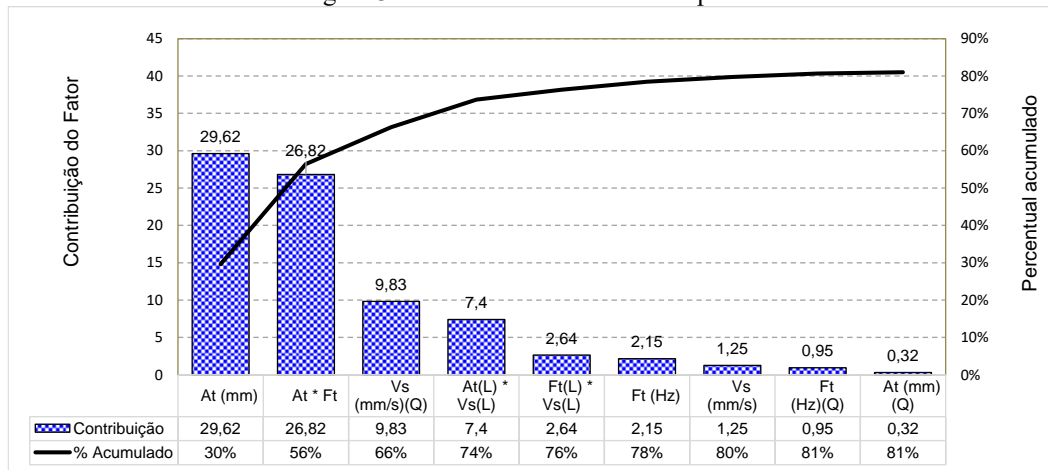
The data collected from the height and width of the weld bead, the dilution values for each treatment of the matrix of BBD experiments can be observed in Figure 2. It is possible to notice low dilution and width values that exceed 22 mm, as well as minimum reinforcement heights of 3.62 mm. The highest dilution value presented did not exceed 8%. The coefficient of determination ( $R^2$ ) of each and every model must be estimated in order to know the experimental and statistical fit of the model obtained. The  $R^2$  values of the responses analyzed were: 81% (dilution), 83% (reinforcement height) and the highest of all observed, 88% for width. These values are considered satisfactory in the analysis of the mathematical/statistical model, since the minimum value is 70% (MONTGOMERY, 2007). This shows that the dilution control, even if considered adjusted, had the lowest adjustment in relation to the bead morphology, and is also the only variable that involves metallurgical issues.

Figure 2: Reinforcement height, width, and dilution values of the experimental matrix.



By means of ANOVA, it was possible to determine that the main parameters At and Ft have a strong significant effect on dilution to a significance level  $\alpha = 0.05$  (p-value < 0.05). Figure 3 shows that the weaving amplitude has a contribution of 29.62%, while its linear interaction with the weaving frequency has a contribution of 26.82%, showing that together they correspond to more than 50% of weight. The statistical error was 7.39%, the highest among the response variables analyzed.

Figure 3: Pareto chart for dilution response.



As the contribution of weaving amplitude and frequency are relevant, Figure 4 shows the behavior of this interaction in relation to the dilution studied. The behavior of frequency and amplitude at the maximum values showed an unfavorable result for dilution, since it presented high values, above 7%. The weaving amplitude values at the low value, at 6 mm, showed excellent dilution values, regardless of the weaving frequency used.

In addition, the optimal combination for minimum dilution values in the analyzed crop points to minimum values of At and maximum Ft, even though this relationship is not directly tested in the experimental matrix by the inherent characteristic of BBD. The weaving amplitude being the most influential input variable goes according to the dilution response, since At increases, increases the width and also the dilution value (PIMENTEL, 2023).

Figure 4:  $F_t$  versus  $A_t$  interaction for dilution.

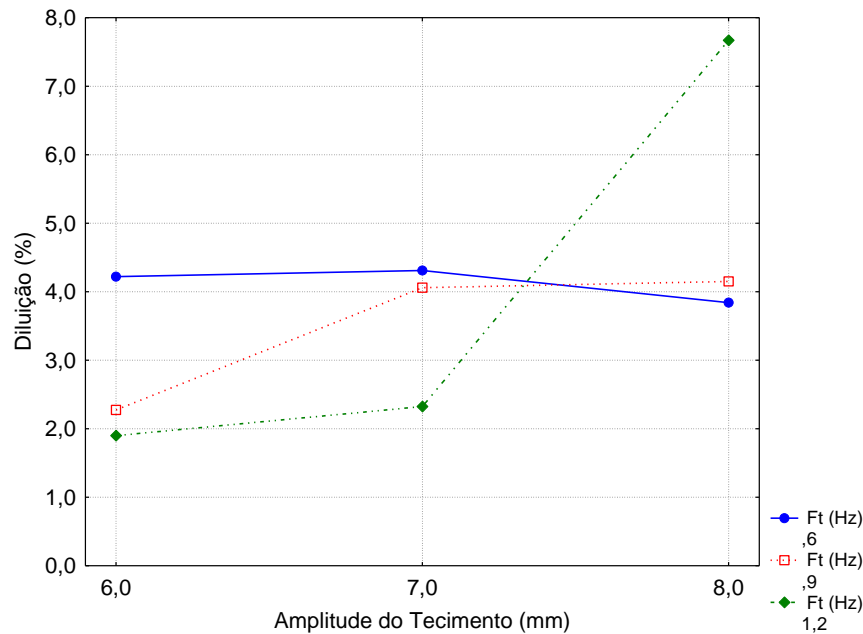
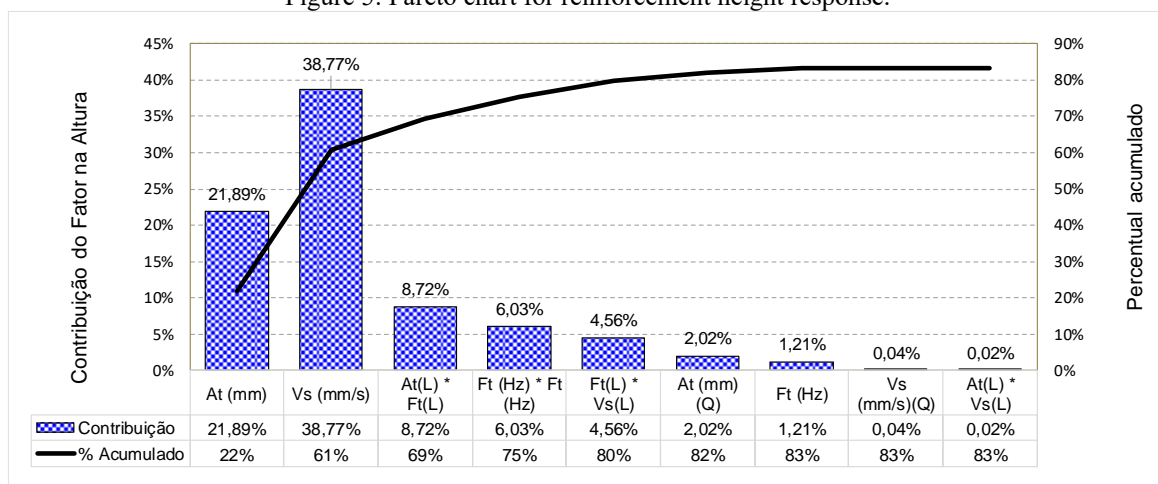


Figure 5 shows the Pareto chart for reinforcement height response. Through an analysis based on ANOVA, it is possible to observe the main contribution parameters, in which they showed a contribution of 38.77% for  $V_s$  and 21.89% for TA, both adding up to 61%. The error for the reinforcement height response was 4.68%. It can be noted that unlike dilution, the linear of significant contribution is seen in two input parameters, including a high contribution of welding speed being more prominent.

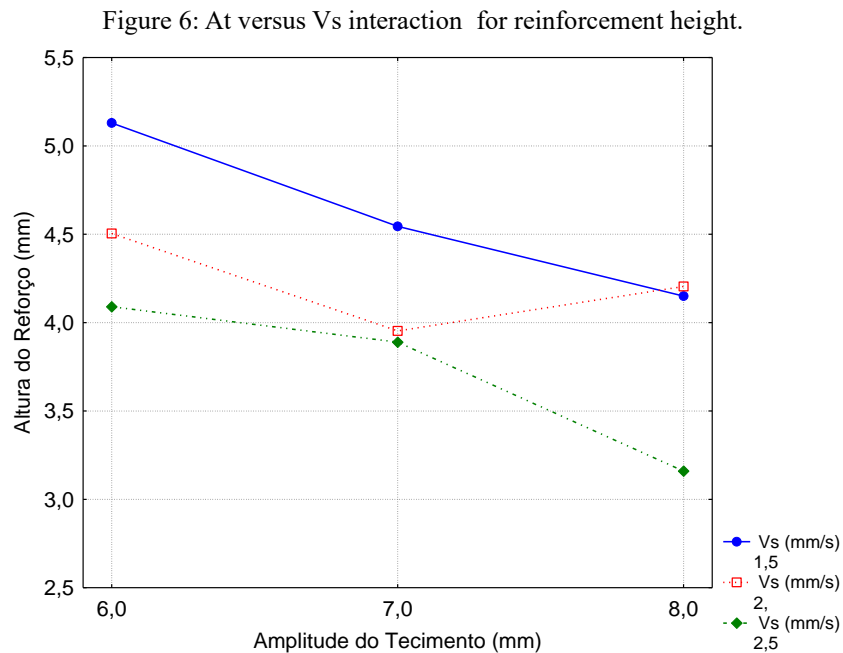
Figure 5: Pareto chart for reinforcement height response.



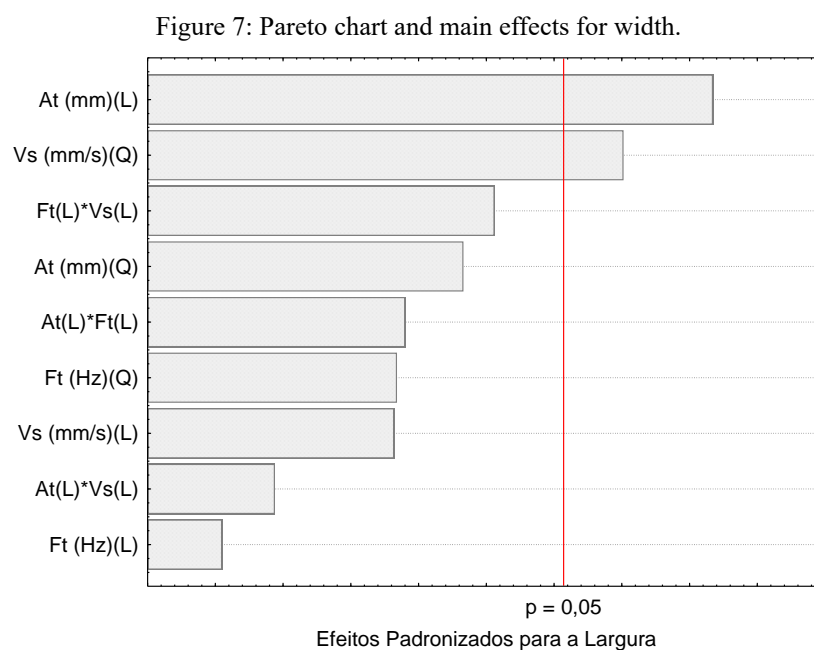
With the significant parameters seen in ANOVA, with Figure 6 it is possible to understand the behavior of the variables with the greatest contribution. It is possible to notice that as the weaving amplitude increases, the reinforcement height decreases, for all levels of  $V_s$ . The welding speed



values at the low level show higher values of reinforcement height, with a response greater than 5 mm of reinforcement height for low levels of  $A_t$  and  $V_s$ .



By means of ANOVA, the main parameters were determined, significant for a significance level  $\alpha = 0.05$  ( $p$ -value  $< 0.05$ ). By means of the Pareto chart, in Figure 7, it is possible to observe that  $A_t$  (L) and  $V_s$  (Q) are significant, with a contribution of 32.08 % for the first and 21.58 % for the second. In addition to presenting an error of 5.36% for width, both factors contribute more than 50%, showing the impact of the parameters.



It is possible to notice the behavior of the significant variables in Figure 8, where no curve intersects, showing an increasing behavior for all  $V_s$ , as the value of  $A_t$  goes from the low to the high level. It is possible to achieve values greater than 20 mm in width with the combination of  $A_t (+1)$  and  $V_s (0)$ . When searching for minimum width values, values of  $A_t (-1)$  and  $V_s (+1)$  should be entered, reaching a value of 14 mm.

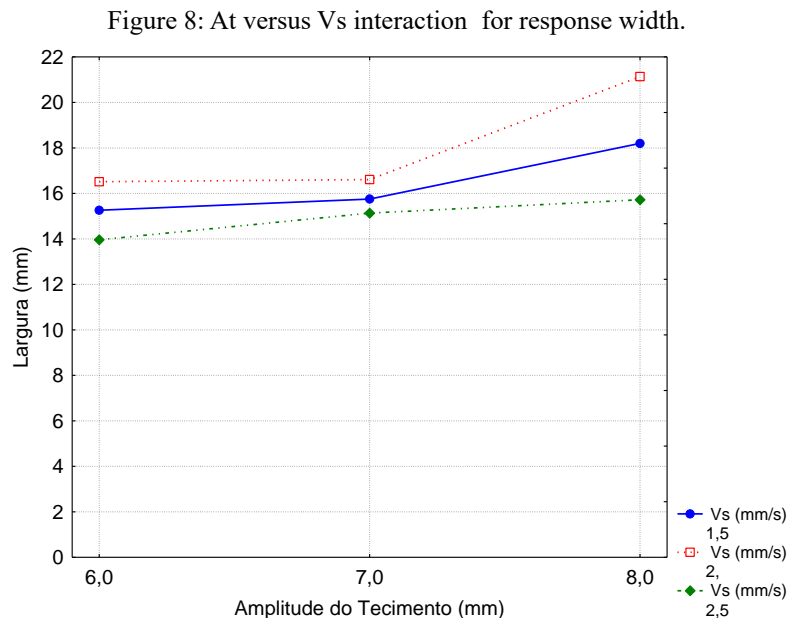
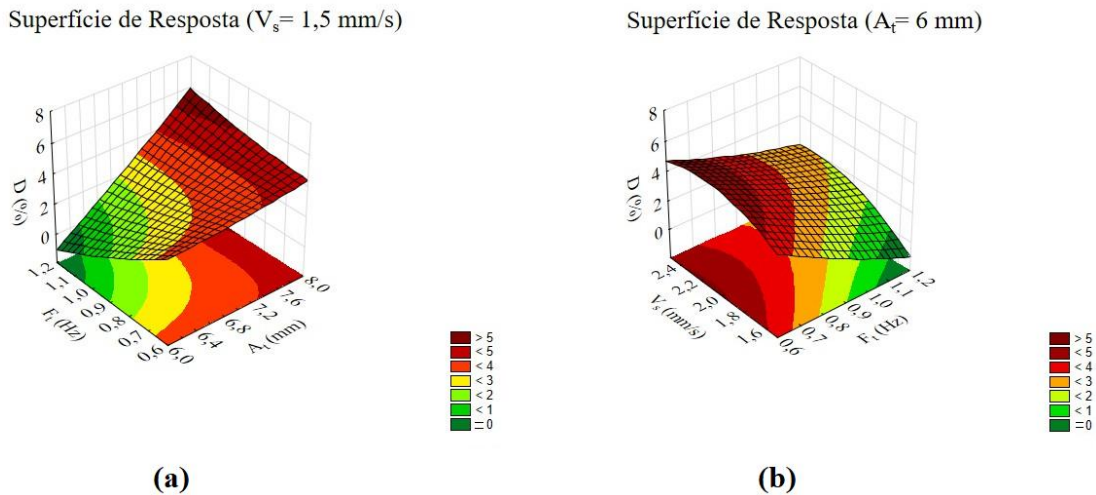


Figure 9 (a) shows the response with a value of  $V_s (-1)$ , as it presented the lowest dilution response, being beneficial for coating (GOMES, 2010; PIMENTEL, 2023), as well as the  $A_t * F_t$  ratio proved to be influential, as seen in the Pareto chart in Figure 3. It can be seen that, even if the response values do not present a concave, convex or saddle morphology (BEZERRA ET AL., 2008; BOX AND DRAPER, 2007; EDWARDS, 2007; OLIVEIRA, 2018), a morphology similar to convex can be observed, with the minimum point being eligible.

The morphology shows that the proposed experimental arrangement presented the possibility of obtaining minimum values, even though it was not a well-characterized surface with a convex shape. With  $A_t (-1)$  and  $F_t (+1)$  values, it is possible to obtain minimum dilution values, much lower than those referenced (MURUGAN AND PARMAR, 1997). Even if the values fluctuate in any axis, the dilution still presents low values, applicable to coating.

Figure 9 (b) shows the response surface of  $F_t * V_s$ , which is significant as Figure 3 shows an  $A_t (-1)$  value, since its individual response has a lower dilution value. It can be noted that the minimum dilution value is obtained with  $F_t (+1)$  and  $V_s (-1)$  values, in a format conducive to presenting a minimum point, within a well-established arrangement without stratopulation, but different from a convex point. In addition, in both graphs in Figure 9, it is possible to notice targets of achievable values with zero dilution, both in (a) and (b).

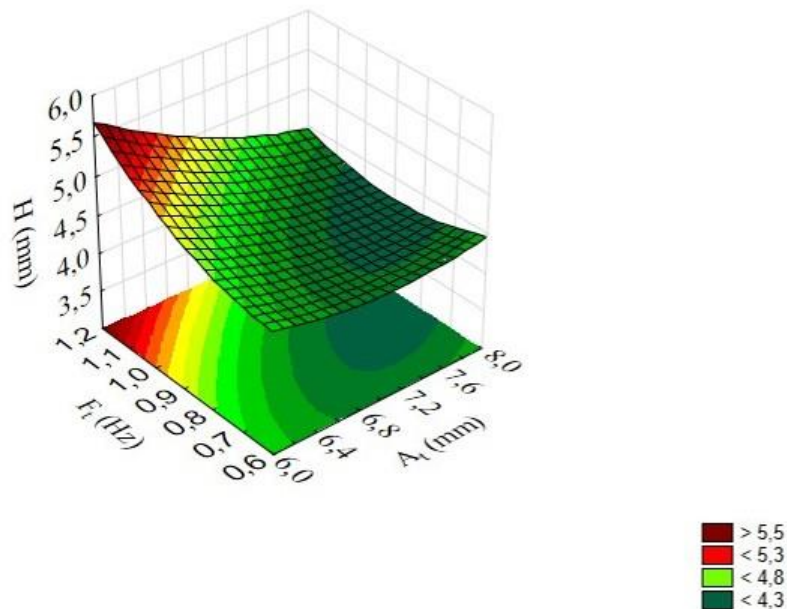
Figure 9: (a) MSR  $F_t$  versus  $A_t$  with  $V_s=1.5$  mm/s, for dilution; (b) MSR  $V_s$  versus  $F_t$  with  $A_t=6$  mm, for dilution.



Considering the influential values in the Pareto chart in Figure 5, Figure 10 shows the ratio of  $A_t * F_t$  with  $V_s$  (-1), as it presents the highest reinforcement height response, which is beneficial for coating (PIMENTEL, 2023). With it, it can be seen that with the shape of the MSR a well-defined maximum point is now achieved, even if it is not a convex surface, reaching values greater than 5.5 mm of reinforcement height with  $A_t$  (-1) and  $F_t$  (+1). Even at the lower values of reinforcement height, it presented a satisfactory value, meeting coating projects (MOTA ET AL., 2016).

Figure 10: MSR  $F_t$  versus  $A_t$  with  $V_s=1.5$  mm/s, for reinforcement height.

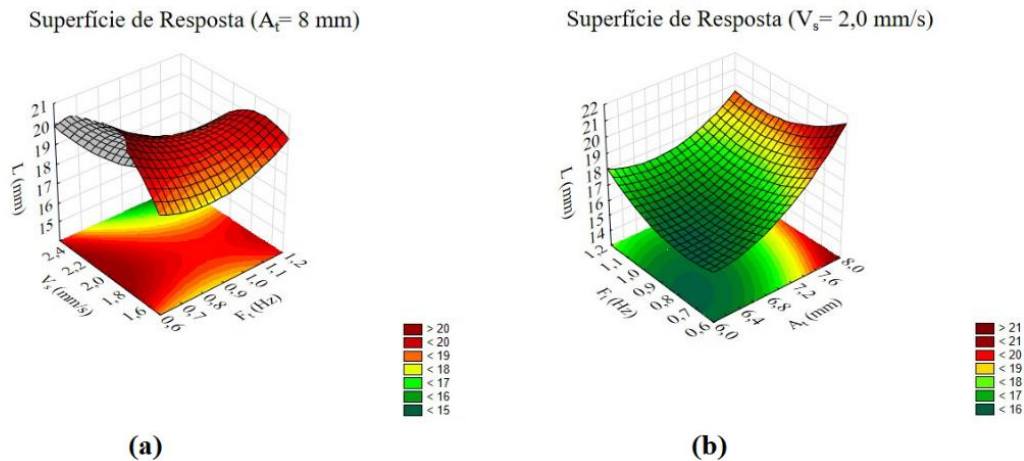
Superfície de Resposta ( $V_s = 1,5$  mm/s)



By means of the influential values in the Pareto plot in Figure 7, Figure 11 (a) presents  $A_t$  (+1), as it returns the largest width value, having a saddle surface as a response, which usually for maximum point optimization presents multiple results, as most studies (OLIVEIRA, 2018). However,

the minimum point values are practically unfeasible, given their morphology. Even so, the width values present a large coverage region with values greater than 20 mm, especially in the central part of the response.

Figure 11: (a) MSR  $V_s$  versus  $F_t$  with  $A_t = 8$  mm, for bead width; (b) MSR  $F_t$  versus  $A_t$  with  $V_s = 2.0$  mm/s, for bead width.



However, in Figure 11 (b), with  $V_s$  (0), it presents the greatest width, as seen in Figure 7. Even though it does not have a concave surface, it is possible to observe a region of maximum point, with values of  $A_t$  (+1) and  $F_t$  (-1), reaching values greater than 21 mm, higher than coating with other welding processes that used weaving (PIMENTEL, 2023). Even with the minimum response values, in the green region, high width values are still possible, largely due to the use of weaving.

As optimization depends on multi-response, i.e., the input variables must be resized, still within the experimental arrangement, since the returned values found meet the project. Thus, the use of optimization is common to achieve a specific objective, or a series of them (PAIVA ET AL., 2007). Figure 12 (b) shows the optimization with the method proposed by (DERRINGER AND SUICH, 1980), where it presented both simple and compound desirability maximums, showing a probable range.

Also in Figure 12 (b) it is possible to notice that the values of the optimized multi-response, where they present a response of: weaving amplitude 6.0 mm, weaving frequency 1.20 Hz and welding speed 1.50 mm/s. This demonstrates that the optimization values are at the minimum extremes of the experimental arrangement for  $A_t$  and  $V_s$ , and maximum for  $F_t$ . The maximum reinforcement height value was 5.67 mm, which demonstrates a bead eligible for coating application, without the use of vertical overlap (SILVA ET AL., 2014).

Figure 12: (a) optimized cords; (b) optimization via desirability method.

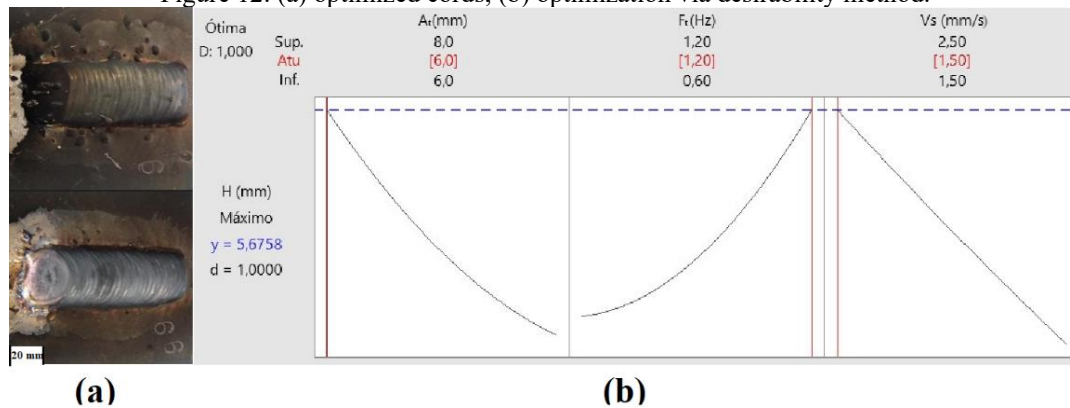


Figure 12 (a) shows the morphology of the two strands optimized to obtain the experimental error, using the reinforcement height value. In addition to presenting a good continuity, without the presence of pores, it is possible to see a good repetitiveness. The optimization error showed a value of 8.8%, even lower than in coating, with another process, but with the same pair of materials, with the use of BBD and optimization via desirability (PIMENTEL, 2023; PIMENTEL ET AL., 2023).

## CONCLUSIONS

With the present work, it was possible to conclude:

- The MIG-PV process showed good geometric continuity, adequate bead morphology, as well as low dilutions that credit it to the application in coating.
- The R2 values showed an excellent fit, with a lower value of 81% for dilution and a maximum of 88% for width.
- Via ANOVA for dilution,  $A_t$  was more significant with a value of 29.62% and an error of 7.39% for the response.
- Via ANOVA for reinforcement height,  $V_s$  was more significant with a value of 38.77% and an error of 4.68% for the response.
- Via ANOVA for width,  $A_t$  was more significant with a value of 32.08% and an error of 5.36% for the response.
- The optimization via the proposed desirability method with a maximum value had a return ( $y$ ) of 5.67 mm. The system fed back the input aiming at optimization with values  $A_t$  (-1) and  $V_s$  (-1) and  $F_t$  (+1).
- The proposed experimental error via desirability showed a mean value of 8.8%.



## REFERENCES

1. Abuhabaya, A., Fieldhouse, J., & Brown, D. (2013). The optimization of biodiesel production by using response surface methodology and its effect on compression ignition engine. *\*Fuel Processing Technology\**, 113, 57-62.
2. Ahmadnia, M., Shahraki, S., & Kamarposhti, M. A. (2016). Experimental studies on optimized mechanical properties while dissimilar joining AA6061 and AA5010 in a friction stir welding process. *\*International Journal of Advanced Manufacturing Technology\**, 87(5-8), 2337–2352.
3. Augustin, G., Davila, S., Udilljak, T., Staroveski, T., Brezak, D., & Babic, S. (2012). Temperature changes during cortical bone drilling with a newly designed step drill and an internally cooled drill. *\*International Orthopaedics\**, 36(7), 1449-1456.
4. Bezerra, M. A., Santelli, R. E., Oliveira, E. P., Villar, L. S., & Escalera, L. A. (2008). Response surface methodology (RSM) as a tool for optimization in analytical chemistry. *\*Talanta\**, 76, 965-977.
5. Box, G. E. P., & Hunter, J. S. (1961). The 2k-p Fractional Factorial Designs Part. *\*Technometrics\**, 3(3), 311-351.
6. Box, G. E. P. (1954). Exploration and Exploitation of Response Surfaces: Some General Considerations and Examples. *\*Biometrics\**, 10(1), 16-60.
7. Box, G. E. P., & Behnken, D. W. (1960). Some new three level designs for the study of quantitative variables. *\*Technometrics\**, 2(4), 455-475.
8. Box, G. E. P., & Draper, N. R. (1987). *\*Empirical model building and response surfaces\**. New York: John Wiley & Sons, Inc.
9. Box, G. E. P., & Draper, N. R. (2007). *\*Response surfaces, mixtures, and ridge analyses\** (2nd ed.). Hoboken: John Wiley & Sons.
10. Brightman, H. J. (1978). Optimization through experimentation: applying Response Surface Methodology. *\*Decision Sciences\**, 9(3), 481-495.
11. Deb, K., Sindhya, K., & Hakanen, J. (2017). Multi-Objective Optimization. In R. N. Sengupta, A. Gupta, & J. Dutta (Eds.), *\*Decision Sciences: Theory and Practice\** (pp. 146-179). Boca Raton: Taylor and Francis.
12. Derringer, G., & Suich, R. (1980). Simultaneous Optimization of Several Response Variables. *\*Journal of Quality Technology\**, 12(4), 214-219.
13. Edwards, J. R. (2007). Polynomial regression and response surface methodology. In C. Ostroff & T. A. Judge (Eds.), *\*Perspectives on organizational fit\** (pp. 361-372). San Francisco: Jossey-Bass.
14. Ekici, E., & Motorcu, A. R. (2014). Evaluation of drilling Al/SiC composites with cryogenically treated HSS drills. *\*International Journal of Advanced Manufacturing Technology\**, 74(9), 1495-1505.



15. Farias, J. P., Miranda, H. C., Motta, M. F., Paiva, F. D. Q., & Pessoa, E. F. (2005). Efeito da Soldagem MIG/MAG em Corrente Alternada sobre a Geometria da Solda. *\*Soldagem & Inspeção\**, 10(4), 173-181.
16. Fratari, R. Q., Schwartzman, M. A. M., & Scotti, A. (2010). Otimização dos parâmetros de tecimento para confecção de amanteigamento em chapas de aço ao carbono pelo processo TIG com arame AWS ER309L. *\*Soldagem & Inspeção\**.
17. Ghaedi, M., Hajjati, S., Mahmudi, Z., Tyagi, I., Agarwal, S., Maity, A., & Gupta, V. K. (2015). Modeling of competitive ultrasonic assisted removal of the dyes - Methylene blue and Safranin-O using Fe<sub>3</sub>O<sub>4</sub> nanoparticles. *\*Chemical Engineering Journal\**, 268, 28-37.
18. Gomes, J. H. F. (2010). *\*Análise e otimização da soldagem de revestimento de chapas de aço ABNT 1020 com utilização de arame tubular inoxidável austenítico\** (Dissertação de Mestrado em Engenharia de Produção, Universidade Federal de Itajubá).
19. Goos, P., & Jones, B. (2011). *\*Optimal Design of Experiments: a case study approach\**. Chichester: John Wiley & Sons.
20. Hasan, M. M., Ishak, M., & Rejab, M. R. M. (2017). Influence of machine variables and tool profile on the tensile strength of dissimilar AA7075-AA6061 friction stir welds. *\*International Journal of Advanced Manufacturing Technology\**, 90(9-12), 2605-2615.
21. Hosseinzadeh, M., & Mouziraji, M. G. (2016). An analysis of tube drawing process used to produce squared sections from round tubes through FE simulation and response surface methodology. *\*International Journal of Advanced Manufacturing Technology\**, 87(5-8), 2179-2194.
22. Jahanzaib, M., Hussain, S., Wasim, A., Aziz, H., Mirza, A., & Ullah, S. (2017). Modeling of weld bead geometry on HSLA steel using response surface methodology. *\*International Journal of Advanced Manufacturing Technology\**, 89(5-8), 2087-2098.
23. Kannan, T., & Yoganandh, J. (2010). Effect of process parameters on clad bead geometry and its shape relationships of stainless steel claddings deposited by GMAW. *\*International Journal of Advanced Manufacturing Technology\**, 47, 1083-1095.
24. Kant, G., & Sangwan, K. S. (2014). Prediction and optimization of machining parameters for minimizing power consumption and surface roughness in machining. *\*Journal of Cleaner Production\**, 83, 151-164.
25. Korra, N. N., Vasudevan, M., & Balasubramanian, K. R. (2015). Multi-objective optimization of activated tungsten inert gas welding of duplex stainless steel using response surface methodology. *\*International Journal of Advanced Manufacturing Technology\**, 77(1-4), 67-81.
26. Kumar, N., Mukherjee, M., & Bandyopadhyay, A. (2017). Comparative study of pulsed Nd:YAG laser welding of AISI 304 and AISI 316 stainless steels. *\*Optics & Laser Technology\**, 88, 24-39.
27. Hoerl, R. W. (1985). Ridge Analysis 25 Years Later. *\*The American Statistician\**, 39(3), 186-192.
28. Leithold, L. (1994). *\*O cálculo com geometria analítica\** (3<sup>a</sup> ed.). São Paulo: HARBRA.



29. Lotfi, A. H., & Nourouzi, S. (2014). Predictions of the optimized friction stir welding process parameters for joining AA7075-T6 aluminum alloy using preheating system. *\*International Journal of Advanced Manufacturing Technology\**, 73(9-12), 1717-1737.
30. Miranda, E. C., Silva, C. C., Motta, M. F., Miranda, H. C., & Farias, J. P. (2015). Avaliação do Uso do Tecimento sobre o Nível de Diluição e Geometria do Cordão de Solda na Soldagem TIG com Alimentação Automática de Arame Frio. *\*Soldagem & Inspeção\**, 180-190.
31. Montgomery, D. C. (2007). *\*Applied Statistics and Probability for Engineers\** (4th ed.). Hoboken: John Wiley & Sons.
32. Montgomery, D. C. (2017). *\*Designs and Analysis of Experiments\** (9th ed.). USA: John Wiley & Sons.
33. Mostaan, H., Shamanian, M., & Safari, M. (2016). Process analysis and optimization for fracture stress of electron beam welded ultra-thin FeCo-V foils. *\*International Journal of Advanced Manufacturing Technology\**, 87(1-4), 1045–1056.
34. Mostafapour, A., Ebrahimpour, A., & Saeid, T. (2017). Finite element investigation on the effect of FSSW parameters on the size of welding subdivided zones in TRIP steels. *\*International Journal of Advanced Manufacturing Technology\**, 88(1-4), 277–289.
35. Mota, C. A. M., Nascimento, A. S., Garcia, D. V., Silva, F. R. T., & Ferraresi, V. A. (2016). Revestimento de Níquel Depositado pela Soldagem MIG e MIG com Arame Frio. *\*Soldagem & Inspeção\**, 21(4), 483-496.
36. Murugan, N., & Parmar, R. S. (1994). Effects of MIG process parameters on the geometry of the bead in the automatic surfacing of stainless steel. *\*Journal of Materials Processing Technology\**, 41, 381-398.
37. Murugan, N., & Parmar, R. S. (1997). Stainless steel cladding deposited by automatic gas metal arc welding. *\*Welding Journal\**, 76, 391s-403s.
38. Myers, R. H., & Montgomery, D. C. (2009). *\*Response Surface Methodology: process and product optimization using designed experiments\** (3rd ed.). New York: John Wiley & Sons.
39. Nascimento, A. S., Fernandes, D. B., Mota, C. A. M., & Vilarinho, L. O. (2009). Methodology for determination of parameters for welding MIG with variable polarity. *\*Welding International\**, 473-480.
40. Öktem, H., Erzurumlu, T., & Kurtaran, H. (2005). Application of response surface methodology in the optimization of cutting conditions for surface roughness. *\*Journal of Materials Processing Technology\**, 170(1-2), 11-16.
41. Oliveira, L. G. de. (2018). *\*Fundamentos da Metodologia de Superfície de Resposta e suas aplicações em Manufatura Avançada: Uma análise crítica\** (Dissertação de Mestrado, Universidade Federal de Itajubá).
42. Paiva, A. P., Ferreira, J. R., & Balestrassi, P. P. (2007). A multivariate hybrid approach applied to AISI 52100 hardened steel turning optimization. *\*Journal of Materials Processing Technology\**, 189, 26-35.





43. Patel, M. G. C., Krishna, P., & Parappagoudar, M. B. (2016). An intelligent system for squeeze casting process – soft computing based approach. *\*International Journal of Advanced Manufacturing Technology\**, 86(9), 3051-3065.
44. Pimentel, R. E. (2023). Revestimento de AWS A5.9 ER385 (AISI 904L) pelo processo TIG-P arame frio em ASTM A36. *\*Programa de Pós-Graduação em Engenharia Mecânica (PROMEC)\**. Universidade Federal do Rio Grande do Sul (UFRGS).
45. Pimentel, R. E., Gonzalez, A. R., Botega, M., & Marcolin, V. C. (2023). Aplicação de BBD em revestimento por soldagem TIG-P com tecimento. *\*RevistaFT\**, Edição 125, Vol. 27, Pag. 9-10.
46. Puhl, E. B. (2011). Desenvolvimento de tecnologias no processo MIG/MAG para aumento de produtividade e melhoria da qualidade mediante o uso da polaridade negativa. *Dissertação (Mestrado em Engenharia Mecânica) - Universidade Federal de Santa Catarina, Florianópolis*.
47. Ramachandran, K. K., Murugan, N., & Kumar, S. Shashi. (2016). Performance analysis of dissimilar friction stir welded aluminium alloy AA5052 and HSLA steel butt joints using response surface method. *\*International Journal of Advanced Manufacturing Technology\**, 86(9-12), 2373–2392.
48. Rao, S. S. (2009). *\*Engineering optimization: theory and practice\** (4th ed.). Hoboken: John Wiley & Sons.
49. Roshan, Babajanzade S., Jooibari, Behboodi M., Teimouri, R., Asgharzadeh-Ahmadi, G., Falahati-Naghbi, M., & Sohrabpoor, H. (2013). Optimization of friction stir welding process of AA7075 aluminum alloy to achieve desirable mechanical properties using ANFIS models and simulated annealing algorithm. *\*International Journal of Advanced Manufacturing Technology\**, 69(5-8), 1803-1818.
50. Safeen, W., Hussain, S., Wasim, A., Jahanzaib, M., Aziz, H., & Abdalla, H. (2016). Predicting the tensile strength, impact toughness, and hardness of friction stir-welded AA6061-T6 using response surface methodology. *\*International Journal of Advanced Manufacturing Technology\**, 87, 1765-81.
51. Šaparauskas, J., Zavadskas, E. K., & Turskis, Z. (2011). Selection of facade's alternatives of commercial and public buildings based on multiple criteria. *\*International Journal of Strategic Property Management\**, 15(2), 189–203.
52. Senthilkumar, B., & Kannan, T. (2015). Effect of flux cored arc welding process parameters on bead geometry in super duplex stainless steel claddings. *\*Measurement\**, 62, 127-136.
53. Shi, H., Zhang, K., Xu, Z., Huang, T., Fan, L., & Bao, W. (2014). Applying statistical models optimize the process of multi-pass narrow-gap laser welding with filler wire. *\*International Journal of Advanced Manufacturing Technology\**, 75(1-4), 279–291.
54. Silva, C. C., Afonso, C. R. M., Ramirez, A. J., Motta, M. F., Miranda, H. F., & Farias, J. P. (2014). Evaluation of the Corrosion Resistant Weld Cladding Deposited by the TIG Cold Wire Feed Process. *\*Mat. Science For.\**, 2822-2827.
55. Sivarao, Milkeya, K. R., Samsudina, A. R., Dubeyb, A. K., & Kidde, P. (2014). Comparison between Taguchi Method and Response Surface Methodology (RSM) in Modelling CO2 Laser Machining. *\*Jordan Journal of Mechanical and Industrial Engineering\**, 8(1), 35-42.



56. Song, X., Zhang, M., Pei, Z. J., & Wang, D. (2014). Ultrasonic vibration-assisted pelleting of wheat straw: A predictive model for energy consumption using response surface methodology. *\*Ultrasonics\**, 54(1), 305-311.
57. Stewart, J. (2012). *\*Calculus\** (7th ed.). Belmont: Cengage.
58. Sudhagar, S., Sakthivel, M., Mathew, Prince J., & Daniel, S. A. A. (2017). A multi-criteria decision making approach for process improvement in friction stir welding of aluminium alloy. *\*Measurement\**, 108, 1-8.
59. Teimouri, R., Amini, S., & Mohagheghian, N. (2017). Experimental study and empirical analysis on effect of ultrasonic vibration during rotary turning of aluminum 7075 aerospace alloy. *\*Journal of Manufacturing Processes\**, 26, 1-17.
60. Verma, G. C., Kala, P., & Pandey, P. M. (2017). Experimental investigations into internal magnetic abrasive finishing of pipes. *\*International Journal of Advanced Manufacturing Technology\**, 88, 1657-1668.
61. Zavadskas, E. K., & Turskis, Z. (2010). A new additive ratio assessment (ARAS) method in multicriteria decision-making. *\*Technological and Economic Development of Economy\**, 16(2), 159-172.
62. Winiczenko, R. (2016). Effect of friction welding parameters on the tensile strength and microstructural properties of dissimilar AISI 1020-ASTM A536 joints. *\*International Journal of Advanced Manufacturing Technology\**, 84(5-8), 1657–1668.